

## Assessment of engine noise shielding by the wings of current turbofan aircraft

Alves Vieira, A.E.; Snellen, Mirjam; Simons, Dick G.

**Publication date**

2017

**Document Version**

Final published version

**Published in**

24th International Congress on Sound and Vibration

**Citation (APA)**

Alves Vieira, A. E., Snellen, M., & Simons, D. G. (2017). Assessment of engine noise shielding by the wings of current turbofan aircraft. In B. Gibbs (Ed.), *24th International Congress on Sound and Vibration: London calling 2017* International Institute of Acoustics and Vibration, IIAV.

**Important note**

To cite this publication, please use the final published version (if applicable).  
Please check the document version above.

**Copyright**

Other than for strictly personal use, it is not permitted to download, forward or distribute the text or part of it, without the consent of the author(s) and/or copyright holder(s), unless the work is under an open content license such as Creative Commons.

**Takedown policy**

Please contact us and provide details if you believe this document breaches copyrights.  
We will remove access to the work immediately and investigate your claim.

# ASSESSMENT OF ENGINE NOISE SHIELDING BY THE WINGS OF CURRENT TURBOFAN AIRCRAFT

Ana Vieira, Mirjam Snellen and Dick G. Simons

*Delft University of Technology, Faculty of Aerospace Engineering, Aircraft Noise and Climate Effects Section.  
Kluyverweg 1, 2629 HS. Delft, The Netherlands  
email: A.E.AlvesVieira@tudelft.nl*

The shielding of engine noise by the aircraft wings and fuselage can lead to a significant reduction on perceived noise on ground. Most research on noise shielding is focused on Blended Wing Body (BWB) configurations because of the large dimension of the fuselage. However, noise shielding is also considered relevant in conventional tube and wing configurations when the engines are mounted above the wings. Therefore, it is important to have a noise shielding method adaptable to different aircraft geometries without compromising the accuracy of the predictions or resulting in very slow computations. In this work two methods are used to calculate noise shielding and compared in terms of accuracy and computational time, the Diffraction Integral Method (DIM) and a method built on the Modified Theory of the Physical Optics (MTPO). Both methods are based on the Kirchhoff integral and are considered accurate for sharp-edged objects. It was verified that the two methods are comparable in terms of their predictions, but the MTPO-based method is more efficient computationally. Noise shielding predictions for different frequencies are presented for a flyover of the Fokker 70 considering a realistic geometry and flight conditions. These predictions indicate significant values of noise shielding, which demonstrates its importance in current aircraft.

Keywords: noise shielding, Kirchhoff integral method, Diffraction Integral Method, Modified Theory of Physical Optics

---

## 1. Introduction

Aircraft noise affects the quality of life of more people every day, as air traffic is continuously growing, which can result in negative effects on human health [1]. For that reason noise regulations on airports are strict and institutional noise reduction targets are getting more ambitious.

The engines are still the dominant source of noise in the aircraft, despite the great improvements in turbofan engines since the 60's [2]. The shielding of engine noise by the aircraft airframe can reduce the contribution of the engines to the noise received at the ground, depending on where the engines are located.

The reduction of engine noise due to shielding is considered particularly relevant in Blended Wing Body (BWB) aircraft and most research found in literature is focused on this configuration [3, 4]. The results indicate high levels of noise attenuation due to shielding. These results were validated against experimental data from wind tunnel measurements [5, 6] or by comparison with different computational tools.

Nevertheless, noise shielding can also play an important role in conventional turbofan aircraft, when the engines are located above the wings [7]. In this case, the predictions can be validated

against experimental data of aircraft flyovers under operating conditions [8], which is important to assess the real importance of noise shielding.

Most of the numerical models used to calculate noise shielding are of complex implementation and computationally demanding. In this work two different approaches of the Kirchhoff integral theory are presented, the Diffraction Integral Method (DIM) [9, 7] and a method based on the Modified Theory of Physical Optics (MTPO) [10, 4]. These two methods calculate noise shielding for sharp-edged objects and are comparable in terms of accuracy to more complex methods, such as the Boundary Source Method [11] and the Equivalent Source Method [12], but result in faster predictions for objects of large dimensions, as is the case of an aircraft.

In this research the DIM and the MTPO based method are compared in terms of shielding predictions and computational time for simple cases that can be validated against other noise shielding tools with results available in literature.

Predictions of noise attenuation due to shielding are presented for the Fokker 70, taking into account the realistic geometry and operating conditions, for different source frequencies. These predictions allow one to assess whether noise shielding is expected to have a significant impact in the acoustic signature of this aircraft.

Section 2 presents the theoretical formulation of the DIM and the MTPO based methods. Section 3 gives the comparison of the methods for canonical cases in terms of accuracy of the results and computational time. Section 4 shows the predictions of noise shielding for the Fokker 70 and section 5 summarizes the main conclusions of this paper.

## 2. Theoretical Background

Noise shielding is expected in innovative configurations as the BWB, but also in current aircraft with the engines mounted above the wings. The wings and the fuselage are obstacles between the engines and observers on ground and that results in a reduction of the perceived noise due to the noise shielding.

In conventional aircraft the shielding is affected by the diffraction of engine noise by the wings, which can be approximated as flat plates due to the small dimensions of the airfoil thickness compared with the chord and the span. Therefore, in this case, it is expected that edge-diffracted rays have a more important role than the creeping rays (originated in smooth surfaces, without edges). This is an important assumption when modelling noise shielding because, as a result of this approximation, the complexity and computation time of the solution is reduced.

The Boundary Source Method (BSM) [11] and the Equivalent Source Method (ESM) [12] are considered the most accurate methods for calculating noise shielding, but they are complex to implement and time-consuming. The ray-tracing method [13] is not as complex as the BSM and the ESM but still computationally demanding. The Kirchhoff integral theory is a faster and less complex alternative to those methods, which is based on first principles and accurate for calculating noise shielding for sharp-edged surfaces, as considered in this research.

Consider the situation of Fig. 1, where an arbitrary aperture  $\sigma$  in a screen  $\bar{\sigma}$  is located between a source at position  $\mathbf{x}^Q$  and a receiver position  $\mathbf{x}$ .

The field emitted by the source  $p_i$  and the scattered field  $p_s$ , follow the Helmholtz equation in a volume of control that does not contain the source and the screen surface. The Gauss and Green theorems can be applied to that volume of control and the system of equations is rewritten and simplified by applying approximations on the boundary conditions. It is assumed that the shielding object is at rest and in a non-oscillatory state, meaning that  $p_s$  is zero on the screen. The scattered field  $p_s$  is also assumed to be zero far enough from the source and equal to  $p_i$  in the aperture.

The pressure field at the observer position  $\mathbf{x}$  is then given by the so-called Kirchhoff integral over

the aperture  $\sigma$ ,

$$p_s^{Aperture} = \frac{1}{4\pi} \int_{\sigma} \left[ p_i \mathbf{n} \cdot \nabla \frac{e^{ik|\mathbf{r}|}}{|\mathbf{r}|} - \frac{e^{ik|\mathbf{r}|}}{|\mathbf{r}|} \mathbf{n} \cdot \nabla p_i \right] dS, \quad (1)$$

where  $\mathbf{r} = \mathbf{y} - \mathbf{x}$ ,  $\mathbf{x}$  is the receiver position,  $\mathbf{y}$  is a point in the aperture and  $k$  is the wavenumber.

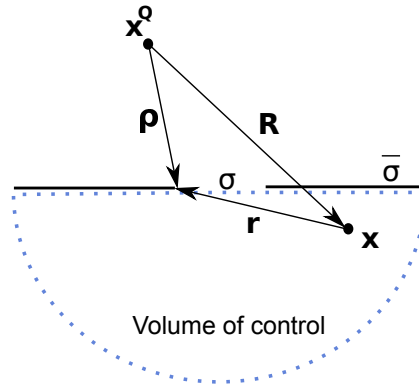


Figure 1: Kirchhoff integration across the circular aperture  $\sigma$  in the screen  $\bar{\sigma}$ .

The calculation of the integral in Eq. 1 is computationally expensive. Therefore the theory of boundary diffracted waves [14] is introduced to simplify the result,

$$p_s = p_{GO} + p_d. \quad (2)$$

Here  $p_d$  is the boundary diffracted field and  $p_{GO} = p_i \chi$ , where  $\chi$  is a unit function equal to unity if the ray source-observer passes through the aperture  $\sigma$ .

Maggi and Rubinowicz [15] obtained an expression for the diffracted field  $p_d$ , which can be written in terms of a line integral along the contour of the aperture  $\partial\sigma$  as,

$$p_d = \frac{A}{4\pi} \oint_{\partial\sigma} \frac{e^{ik|\boldsymbol{\rho}|}}{|\boldsymbol{\rho}|} \frac{e^{ik|\mathbf{r}|}}{|\mathbf{r}|} \frac{(\boldsymbol{\rho} \times \mathbf{r}) \cdot d\mathbf{s}}{|\boldsymbol{\rho}||\mathbf{r}| + \boldsymbol{\rho} \cdot \mathbf{r}}, \quad (3)$$

where  $\boldsymbol{\rho} = \mathbf{x} - \mathbf{x}^Q$  and  $A$  is the strength of the source.

The integral presents a singularity when  $|\boldsymbol{\rho}||\mathbf{r}| + \boldsymbol{\rho} \cdot \mathbf{r} = 0$ , i.e., when the ray between the source and the receiver touches  $\partial\sigma$ . This singularity can be avoided using different approaches. Two methods will be presented in this work, the Diffraction Integral Method (DIM) [7, 9] and a method based on the Modified Theory of Physical Optics (MTPO) [4, 10].

In the DIM, the problem of the singularity was solved by Lummer [3] by subtracting the singularity of the integral and integrating it for a straight line segment of  $\partial\sigma$ , described by,

$$\mathbf{y}(s) = \mathbf{y}_0 + s\mathbf{e}, \quad s_a < s < s_b, \quad (4)$$

where  $\mathbf{y}_0$  is an arbitrary initial point,  $\mathbf{e}$  is the unit direction of the segment and  $s_a$  and  $s_b$  are the start and end points of the segment.

The diffracted field  $p_d$ , considering a monopole source with strength equal to unity, is therefore given by the expression,

$$\begin{aligned} p_d &= \frac{e^{ik|\mathbf{R}|}}{4\pi} \oint_{\partial\sigma} \left[ e^{ik(|\boldsymbol{\rho}|+|\mathbf{r}|-|\mathbf{R}|)} \left( 1 - \frac{\boldsymbol{\rho} \cdot \mathbf{r}}{|\boldsymbol{\rho}||\mathbf{r}|} \right) - 2 \right] \frac{(\boldsymbol{\rho} \times \mathbf{r}) \cdot d\mathbf{s}}{(\boldsymbol{\rho} \times \mathbf{r})^2} + \frac{e^{ik|\mathbf{R}|}}{4\pi} \oint_{\partial\sigma} \frac{2(\boldsymbol{\rho} \cdot \mathbf{r}) \cdot d\mathbf{s}}{(\boldsymbol{\rho} \times \mathbf{r})^2} \quad (5) \\ &= \sum_{I=1}^N (I_1 + I_2). \end{aligned}$$

Here  $N$  is the number of straight segments of  $\partial\sigma$  given by Eq. 4. The terms  $I_1$  and  $I_2$ , using the relations of the Appendix, can be obtained for each segment by

$$I_1 = \frac{e^{ik|\mathbf{R}|\mathbf{u} \cdot \mathbf{e}}}{4\pi} \int_{s_a}^{s_b} \left[ e^{ik(|\rho|+|\mathbf{r}|-|\mathbf{R}|)} \left( 1 - \frac{\rho \cdot \mathbf{r}}{|\rho||\mathbf{r}|} \right) - 2 \right] \quad (6)$$

$$I_2 = \frac{2e^{ik|\mathbf{R}|\mathbf{u} \cdot \mathbf{e}}}{4\pi\|\mathbf{u} \times \mathbf{v}\|} \left[ \tan^{-1} \frac{\mathbf{v} \cdot (\mathbf{v}s - \mathbf{u})}{\|\mathbf{u} \times \mathbf{v}\|} \right]_{s_a}^{s_b} \quad (7)$$

The first integral,  $I_1$ , can be solved using an adaptive quadrature method because of its oscillatory nature. Although the complexity of the Kirchhoff integral is reduced by using the DIM, the integration scheme and the use of symbolic computations still make this method very slow. In addition this method is only valid for monopole sources.

An alternative approach, built on the MTPO, has the same level of accuracy as the DIM and avoids numerical integration, which results in a decreased computational time for the predictions. In addition, in this method, the directivity of the noise source can be considered. For further details about the MTPO-based method consult references [8, 4, 10].

In the MTPO-based method, similarly to the DIM, the aperture contour is discretized in linear edges, and the diffraction potential for each edge is calculated using,

$$I_{\Gamma} = 2\sqrt{\pi}\xi \text{sign}(\xi) F[|\xi|] \{ G(s^*) [U(-\xi_a) - U(-\xi_b) + G(s_a) \text{sign}(\xi_a) F[|\xi_a|] - G(s_b) \text{sign}(\xi_b) F[|\xi_b|]] \}. \quad (8)$$

Here the detour parameter  $\xi(s, P) = \epsilon_{\xi}(P) \sqrt{k[g(s) - |\mathbf{R}|]}$  and  $\epsilon_{\xi}$  is a shadow indicator equal to 1 if the point of the contour  $P$  is located in the illuminated region and -1 if in the shadow,  $\xi_a = \xi(s_a, P)$  and  $\xi_b = \xi(s_b, P)$ .  $F$  is the Fresnel integral,  $U$  is the unit step function and  $s^*$  is the stationary phase point.  $G$  is a function dependent of the amplitude and phase function of the integral of Eq. 3.

The diffracted field through an arbitrary aperture can then be calculated by adding the results of Eq. 8.

The DIM and the MTPO-based method determine the diffracted pressure field  $p_d$  and therefore the scattered field by the aperture is finally calculated using Eq. 2. The scattered field due to the shielding object can be calculated by applying Babinet's principle,

$$p_s^{Object} = p_i - p_s^{Aperture}. \quad (9)$$

The shielding factor,  $\Delta SPL$ , is widely used in literature to quantify noise shielding, and is defined as

$$\Delta SPL = 20 \log_{10} \left| \frac{p_s^{Object}}{p_i} \right|. \quad (10)$$

### 3. Comparison between DIM and the MTPO-based methods

In this section the DIM and the MTPO based method are compared against cases available in literature from other noise shielding methods. The two methods are compared in terms of accuracy and computational time.

Consider the case of a disk, as represented in Fig. 2, which in addition can be considered as representative for a shadow-light limit of a sphere and therefore an approximation of the noise shielding of a sphere without considering the creeping rays.

Consider observers centred in the disk aligned with the  $x$ -axis and that  $a=1$  m. Figs. 3 and 4 show the results of attenuation for  $ka=150$  ( $f=8200$  Hz) and  $ka=200$  ( $f=11000$  Hz) obtained with the DIM and the MTPO-based method. These results show also good agreement with the Fast Scattering Code (FSC) from NASA [12, 7, 4, 8] (not shown here), which is considered a high fidelity method that

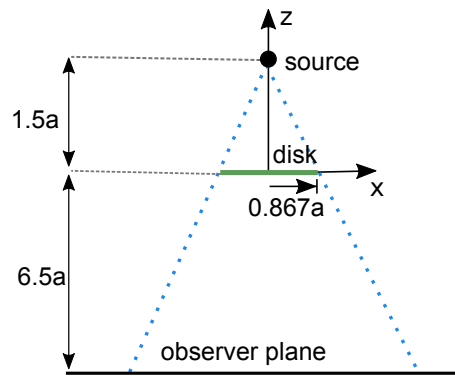
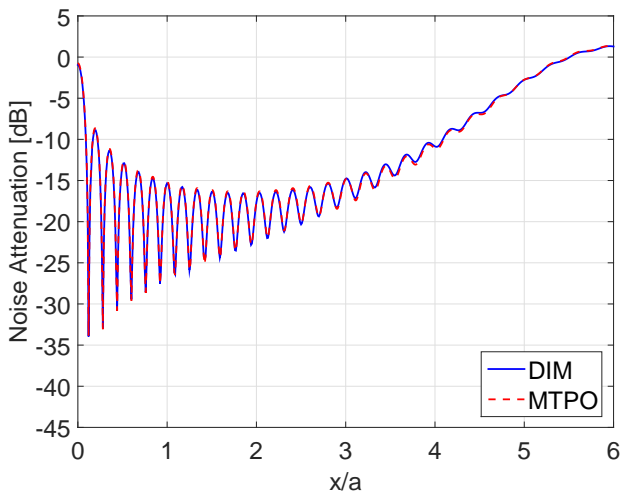
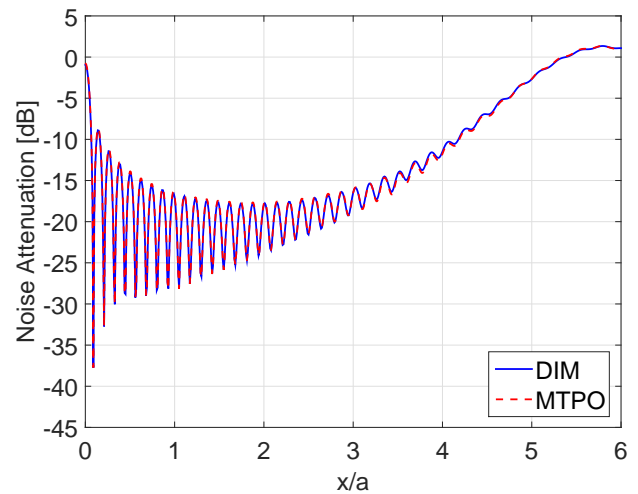


Figure 2: Disk used in the validation of the DIM and the MTPO based method.


 Figure 3: Disk shielding for  $ka=150$ .

 Figure 4: Disk shielding for  $ka=200$ .

uses the Equivalent Source Method. The DIM and the MTPO-based methods show similar results of noise attenuation, despite the differences in computational time, which will be assessed below. Figs. 3 and 4 were obtained using a grid of 750 observer positions on the  $x$ -axis and a discretizations of the contour of the disk of  $\Delta\Phi = 5^\circ$ . In order to obtain feasible results a study of convergence of the results was performed using different discretization of the disk contour. In the convergence study three different source frequencies, 5000 Hz, 8200 Hz and 11000 Hz were considered, and four values of  $\Delta\Phi$ .

It was verified that the discretization of the contour necessary to achieve convergence increases with the frequency, a fact that should be taken into consideration in the analysis. For the frequencies considered, a discretization of  $\Delta\Phi = 10^\circ$  was enough to achieve convergence for a source at 5 000 Hz as can be seen in Fig. 5, but for a source frequency of 11 000 Hz the results only converge for  $\Delta\Phi = 5^\circ$  (Fig. 6).

The MTPO-based method resulted in faster analyses than the DIM. This difference increases as the discretization of the disk contour increases, but it is constant if only the source frequency is changed. In Table 1 the ratio between the computational time used in the DIM and the MTPO-based method is displayed for the different values of  $\Delta\Phi$  considered in the study of convergence. The analysis with the MTPO-based method with  $\Delta\Phi = 20^\circ$  took only 38 s, whereas for the same exact case the DIM took approximately 2 h.

In the case of the disk here considered, the geometry is of small dimensions and a modest number of 750 observer positions is considered. However, when considering a full aircraft and a grid of

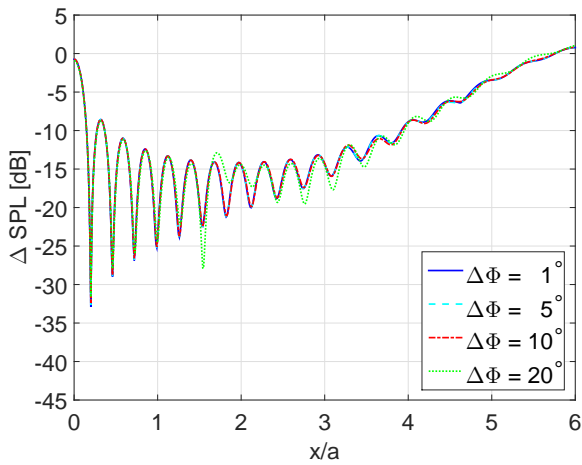
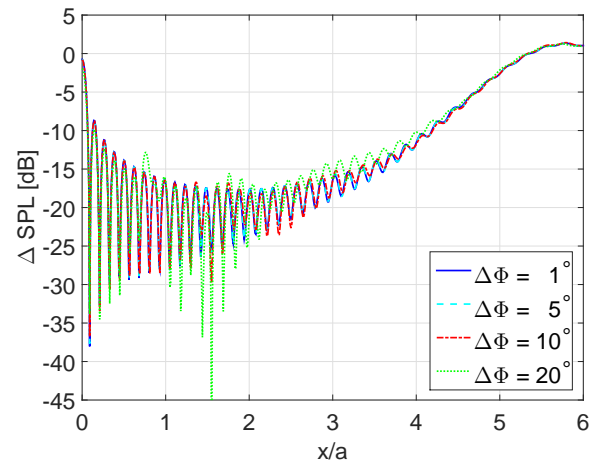

 Figure 5: Study of convergence for  $ka=92$ .

 Figure 6: Study of convergence for  $ka=200$ .

Table 1: Ratio between the computation time of the DIM and the MTPO-based method for the geometry of Fig.2 for different contour discretization.

$\Delta\Phi(^{\circ})$	$t_{DIM}/t_{MTPO}$
20	170
10	270
5	470
1	660

observers the computational time of the simulations will increase drastically. For that reason the MTPO-based method will be adopted in the analysis of the next sections. This method is further compared with other noise shielding methods in [8].

#### 4. Predictions of noise shielding for current aircraft

In this section the MTPO-based method is used to estimate noise shielding for the Fokker 70 (F70). This aircraft was chosen because the wings are very close to the engines (and therefore significant levels of noise attenuation are expected) and it is widely used for short-range flights.

In the predictions a grid of observers is considered below the aircraft at a distance of 64 m and the engines are modelled as monopole sources. The plots of Figs. 7 - 9 represent the variation of SPL due to shielding considering a source frequency of 100 Hz, 2000 Hz and 4000 Hz, respectively.

The plots indicate considerable values of noise attenuation, and such values tend to increase with the frequency of the source, i.e. that the high-frequency range is more attenuated than the low-frequency range, as expected. The plots also show that the area with higher values of attenuation is a projection of the shape of the wings, which depends on the position of the sources.

Considering the values of attenuation per frequency, a significant effect of noise shielding in the F70 acoustic signature is expected. However, one must notice that the individual values of attenuation should be subtracted from the Sound Pressure Level (SPL) for each frequency. For that reason the values of attenuation are not proportional to the noise reduction in the Overall Sound Pressure Level (OSPL).

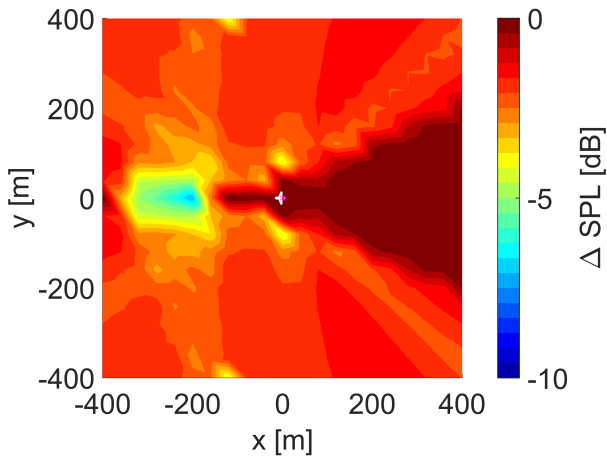


Figure 7: Prediction of noise attenuation of a monopole source at 100 Hz, at the engine position of the Fokker 70 geometry.

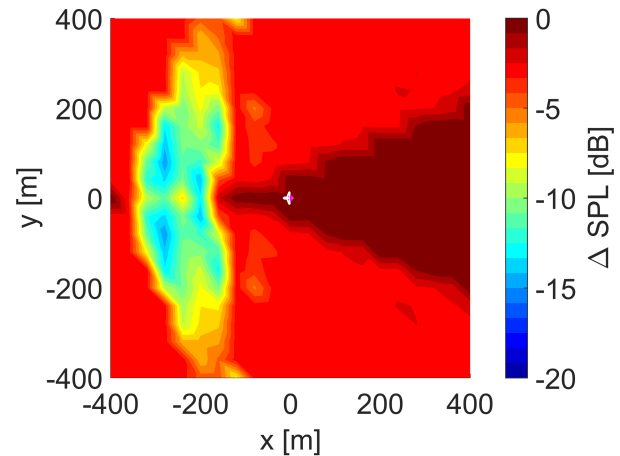


Figure 8: Prediction of noise attenuation of a monopole source at 2000 Hz, at the engine position of the Fokker 70 geometry.

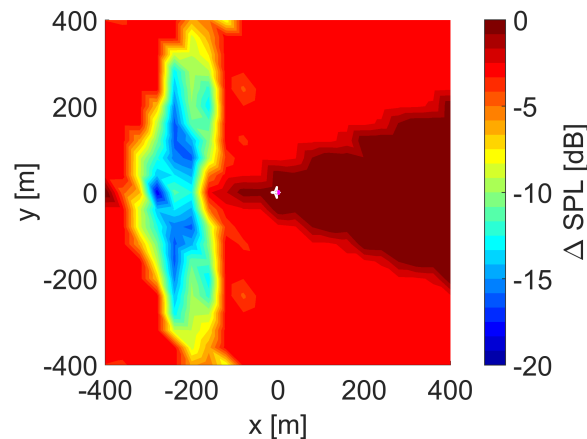


Figure 9: Prediction of noise attenuation of a monopole source at 4000 Hz, at the engine position of the Fokker 70 geometry.

## 5. Summary and Conclusions

In this research two methods for calculating noise shielding for sharp-edged objects were presented, both adequate to be used in conventional turbofan aircraft and BWB configurations. The two methods considered, the DIM and the MTPO-based method, present the same accuracy for sharp-edged objects.

The DIM and the MTPO-based method were compared in terms of computational time and it was shown that the MTPO-based method is much faster and therefore it is preferable for the predictions. A study of convergence showed that the accuracy of the results can be affected by an insufficient discretization of the contour.

The MTPO-based method was used to estimate the noise reduction due to shielding of the engine noise by the fuselage and wings in the case of the Fokker 70. Noise attenuation plots were presented for different source frequencies, and as expected, noise shielding is significant for this aircraft and the noise attenuation values increase with frequency.

## A. Appendix

The integrals of the diffracted field,  $p_d$ , of Eq. 5, can be simplified into Eqs. 6 and 7 using the notation below. This notation was introduced by Lummer [3] to express the discretization of the diffraction problem along a straight line segment.

$$\begin{aligned} \mathbf{y}_0 &= \mathbf{y} - s\mathbf{e}, & \mathbf{a} &= \mathbf{y}_0 - \mathbf{x}^Q, & \mathbf{b} &= \mathbf{y}_0 - \mathbf{x}, & \mathbf{u} &= \mathbf{a} \times \mathbf{b}, & \mathbf{v} &= \mathbf{e} \times (\mathbf{a} - \mathbf{b}) \\ \mathbf{a}^2 &= \mathbf{a} \cdot \mathbf{a}, & \mathbf{b}^2 &= \mathbf{a} \cdot \mathbf{b}, & \alpha &= \mathbf{a} \cdot \mathbf{e}, & \beta &= \mathbf{b} \cdot \mathbf{e}, & \gamma &= \mathbf{a} \cdot \mathbf{b} \\ \boldsymbol{\omega} &= \mathbf{a} \times \mathbf{e}, & \mathbf{z} &= \mathbf{v} + \mathbf{w} \\ \boldsymbol{\rho} &= \mathbf{a} + \mathbf{e}s, & \mathbf{r} &= \mathbf{b} + \mathbf{e}s \\ \boldsymbol{\rho}^2 &= \mathbf{a}^2 + 2\alpha s + s^2, & \mathbf{r}^2 &= \mathbf{b}^2 + 2\beta s + s^2 \\ \boldsymbol{\rho} \cdot \mathbf{r} &= \gamma + (\alpha + \beta)s + s^2, & (\boldsymbol{\rho} \times \mathbf{r}) \cdot d\mathbf{s} &= (\mathbf{a} \times \mathbf{b}) \cdot \mathbf{e}ds \end{aligned}$$

## REFERENCES

1. Lu, C. and Morrell, P. Determination and applications of environmental costs at different sized airports - aircraft noise and engine emissions, *Transportation*, **33**, 45–61, (2006).
2. Huff, D.L. NASA, Noise Reduction Technologies for Turbofan Engines, (2007).
3. Lummer, M. Maggi-Rubinowicz Diffraction Correction for Ray-Tracing Calculations of Engine Noise Shielding, *14th AIAA/CEAS Aeroacoustic Conference, AIAA paper 2008-3050*, (2008).
4. Colas, D.F. and Spakovszky, Z.S. A Turbomachinery Noise Shielding Framework Based on the Modified Theory of Physical Optics, May, 19th AIAA/CEAS Aeroacoustics Conference, (2013).
5. Gerhold, C.H., Clark, L.R., Dunn, M.H. and Tweed, J. Investigation of acoustical shielding by a wedge-shaped airframe, *Journal of Sound and Vibration*, **294**, 49–63, (2006).
6. Reimann, C.A., Tinetti, A.F. and Dunn, M.H. Noise prediction studies for the blended wing body using the fast scattering code, May, 11th AIAA/CEAS Aeroacoustics Conference, (2005).
7. Ng, L.W.T. and Spakovszky, Z. Turbomachinery Noise Shielding Assessment of Advanced Aircraft Configuration, 16th AIAA/CEAS Aeroacoustics Conference, (2010).
8. Vieira, A., Snellen, M. and Simons, D.G. Assessing the engine noise shielding by the wings for current aircraft: a comparison of numerical and experimental approaches, in preparation for The Journal of the Acoustical Society of America.
9. Wai-Tsun Ng, L., *Design and Acoustic Shielding Prediction of Hybrid Wing-Body Aircraft*, Master of Science Thesis, MIT, (2009).
10. Colas, D.F.M., *A Diffraction Integral Based Turbomachinery Noise Shielding Method*, Master of Science Thesis, MIT, (2011).
11. Kirkup, S., *The boundary element method in acoustics, Chap. 1*, Integrated Sound Software (2007).
12. Dunn, M.H. and Tinetti, A. Aeroacoustic scattering via the equivalent source method, May, 10th AIAA/CEAS Aeroacoustics Conference, (2004).
13. Agarwal, A., Dowling, A.P., Ho-Chul, S. and Graham, W. Ray-Tracing Approach to Calculate Acoustic Shielding by a Flying Wing Airframe, *AIAA Journal*, **45** (5), 1080–1090, (2007).
14. Keller, J.B. Geometrical Theory of Diffraction, *Journal of the Optical Society of America*, **52** (2), 116–130, (1962).
15. Miyamoto, K. and Wolf, E. Generalization of the Maggi-Rubinowicz Theory of the Boundary Diffraction Wave - Part I, *Journal of the Optical Society of America*, **52** (6), 615–625, (1962).